Workshop at the University of Tokyo, Japan
23-25. May 2007

COMPONENT CONCEPTS FOR MORPHING STRUCTURES

Wolfgang Luber*
EADS
Military Air Systems OPES
P.O. Box 80 11 60
81663 Munich, Germany

ABSTRACT

As part of the "Advanced Aircraft Structures Program", feasibility studies of different structural concepts of active and morphing structures have been performed. These studies have revealed significant problems related to system complexity and functionality under environmental conditions and severe problems combined with the development of adequate materials.

In the first part, comparison of active smart structure - piezoelectric control systems and aerodynamic active systems for vibration alleviation and elastic mode damping of a military aircraft structure is presented. The vibration alleviation systems which are operative at flight in turbulence or during maneuvers at high incidence reduce severe buffeting levels on the vertical tail structure.

The active systems for elastic mode damping (ASD) are designed as digital systems to provide vibration alleviation and have an interface to the Flight Control System (FCS) or are directly part of the FCS.
The sensor concept of all different systems is the same as the sensor concept used for the FCS with the corresponding benefits of redundancy and safety.
The design of systems and the comparisons of system properties are based on open and closed loop response calculations, performed with the dynamic model of the total aircraft including coupling of flight mechanics, structural dynamics, FCS dynamics and hydraulic actuator or piezo-actuator dynamics.
Aerodynamic systems, like active foreplane and flap concepts, rudder and auxiliary rudder concepts, and piezoelectric systems, like piezo interface at the interconnection fin to rear fuselage and integrated piezo concepts are compared. Besides the essential effects on flexible aircraft mode stability and vibration alleviation factors system complexity and safety aspects are described.

Recently, aerodynamic investigations of adaptive deformable aircraft structures on a scale model of an actual aircraft have been performed with aerodynamic CFD simulations and wind tunnel tests on a complete aircraft model with different shapes of the wing trailing edge. The aerodynamic investigations have shown a considerable drag reduction.

Novel concepts are now under investigation, which might lead to a promising way ahead. One of these concepts uses transversal actuators, which are distributed in the aircraft skin. Detailed analyses of this approach have shown the potential and viability of this approach. Especially it could be shown that the expected weight increase of the adaptive wing structure including actuators is lower than the achieved overall weight decrease of the airplane due to the reduced drag.

NOMENCLATURE

C	unsteady aerodynamic matrix
F	reference area
K	stiffness matrix
M	mass matrix
V	airspeed
b_r	reference length
$\bar{c}, s$	reference length
k	reduced frequency
m_r	reference mass

*Chief engineer Structural Dynamics and Aeroelasticity ,
Email: Wolfgang.Luber@eads.com

q	generalized coordinate
β	sideslip
δ	generalized coordinate
ρ_r	air density
$\rho/2 V^2$	dynamic pressure
ω_r	reference frequency
ω_x	roll rate
ω_z	yaw rate
φ	roll angle
ψ	yaw angle
ξ	differential flap
ζ	rudder
ε	piezo actuator
r	control variables

INTRODUCTION, first part

The development of vibration alleviation control systems for a modern military aircraft as shown in Fig. 1 is strongly influenced by flight mechanic, flight control and aeroservoelastic effects. The flexible aircraft behavior has significant effects on the active vibration alleviation control system. The sensor signals i.e. transducer signals on wing, fuselage and fin and the signals of the Aircraft Motion Sensor Unit (AMSU) - the gyro platform - contain besides the necessary information of rigid aircraft rates and accelerations the flexible aircraft rates and accelerations in the frequencies of the aircraft elastic modes. The 'flexible' accelerations measured by the accelerometers are passed through the active vibration flight control system control paths; they are multiplied by appropriate gains filters and inserted in the control surface actuator (rudder or auxiliary rudder) or integrated piezo, interface actuator inputs. The flexible aircraft is excited by the high frequency actuation inputs and might therefore experience aeroservoelastic instabilities i.e. flutter or limit cycle oscillations, and/or decrease dynamic load and fatigue loads. The adaptive vibration alleviation system design therefore has to minimize all structural coupling effects to avoid aero elastic instabilities through the available means like optimum sensor positioning, notch filtering.

The first part of the paper describes the major aspects, problem areas to be considered in the adaptive system for vibration alleviation (ASD) design with respect to hydraulic and piezoelectric actuator design and total aircraft aeroservoelastic effects, it outlines an integrated design of ASD with FCS. Many of the design and clearance aspects described here have been addressed in previous publications, Ref.'s 1 to 6 for the aircraft with flight control system.

DESIGN OF ACTIVE FLIGHT CONTROL SYSTEM FOR VIBRATION ALLEVIATION

Design philosophy

The design shall include the derivation of adaptive vibration alleviation (ASD) gains, phase advance filters and notch filters to minimize vibrations and dynamic loads on fin, wing and fuselage structure. In addition the structural coupling effects on total aircraft vibration modes shall be minimized in the ASD optimization process. The ASD shall be de-

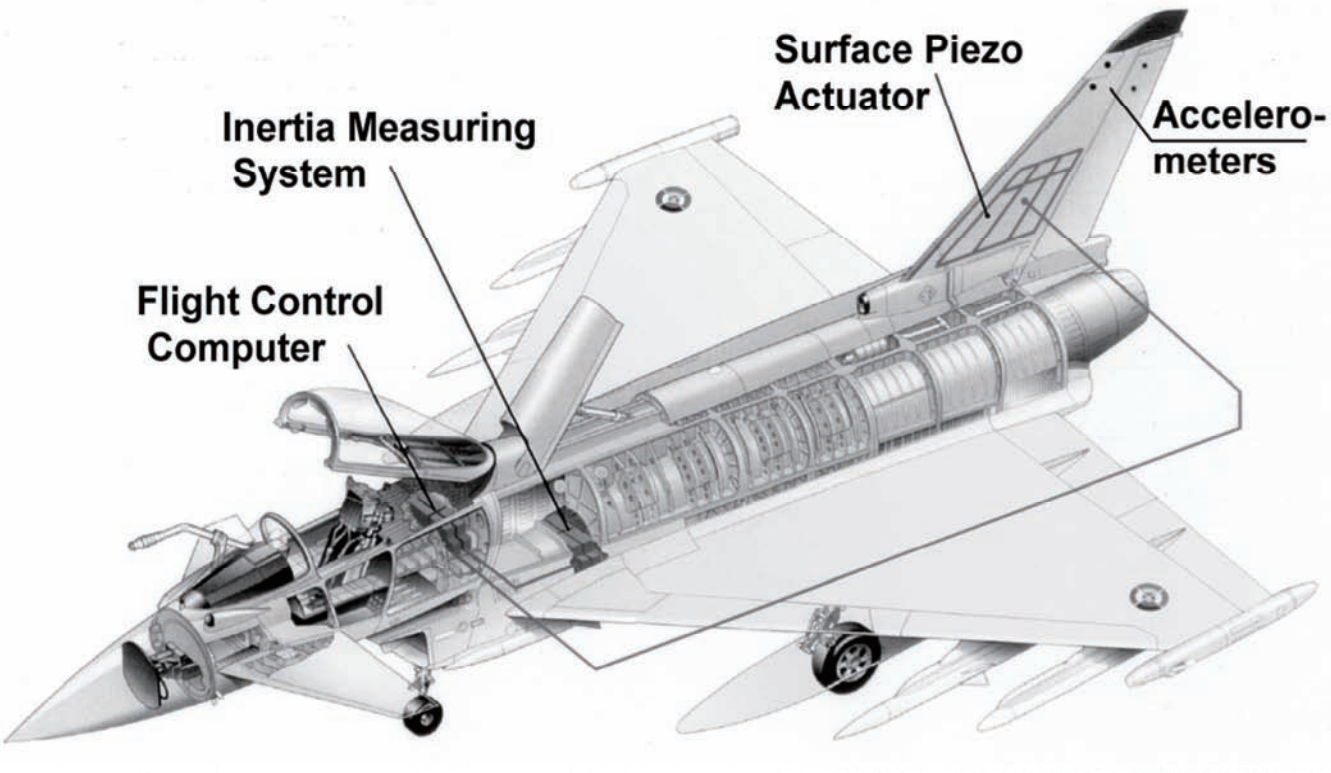

Figure 1: Aircraft with integrated surface piezos

signed to cover the full rigid, flexible aircraft frequency range with respect to aircraft rigid mode and structural mode induced dynamic loads and coupling stability requirements on ground and in flight. The structural coupling influences shall be minimized by ASD and FCS notch filters and notch filters in the wing, fin accelerometer signal feedback signals. The ASD shall be designed to be as robust as possible with respect to all possible aircraft configurations and configuration changes. That includes that all structural changes with configuration should be covered by a constant set of filters to avoid system complexity due to configuration switches for different sets of filters.
In addition scheduling of ASD gains and filters with flight conditions should be introduced to cover the flight envelope. In order to avoid problems in the ASD design due to non-linear unsteady elastic mode and control surface aerodynamics and non-linear piezo-actuator dynamics the elastic mode stability requirements should mainly be based on gain stabilization of the flexible modes. Phase stabilization shall be applied if it can be demonstrated by test.
The ASD design is based upon an analytical model of the total aircraft structure including a linear ASD and FCS model. The analytical model must however be verified through ground test results both from ground resonance and structural coupling testing on aircraft or aircraft components, for example on a component with integrated piezos or with piezo interface. If an ASD demonstrator is envisaged, verification of model technique has to be performed by in flight flutter and structural coupling testing. The model should be updated by the test results for different configurations.

DESIGN REQUIREMENTS

Stability Requirements

The design requirements are primarily stability requirements for all adaptive vibration modes from ASD and flight control rigid/flexible aircraft modes. The stability is achieved by the introduction of notch filters. The Military Specification MIL-F-9490 D for FCS requirements shall be met.

Vibration Alleviation and Dynamic Loads Requirements

The aircraft vibrations on all locations shall meet the requirements of the aircraft without ASD.
The dynamic loads with ASD shall meet the allowable load for the aircraft without ASD for the purpose of increasing the existing incidence range.
The dynamic loads with ASD shall reduce the dynamic loads for the aircraft with ASD for the purpose of increasing the aircraft life cycle.

Flutter Requirements

The FCS design for ASD has to fulfill the flutter requirements of the aircraft without ASD and FCS. The aircraft with ASD and FCS shall meet the 15 % flutter speed margin as well as the minimum elastic mode damping requirements as described in Military Specification MIL-A-8870C.

DESIGN TOOLS

The ASD design for the flexible aircraft is possible with the assumption that the aircraft characteristics are predictable to the necessary accuracy to optimize notch filters which meet the requirements. The characteristics of the controlled flexible aircraft shall be described in the form of open loop frequency transfer functions of the ASD control path feedback loops to a sufficient high frequency, see for example the block diagram in Fig. 2.

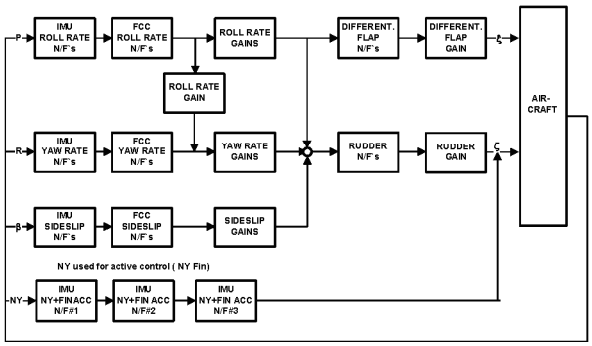

Figure 2: Flow chart for ASD with rudder

For the lateral control the roll rate -, yaw rate-, lateral acceleration - and flow sensor signal β open loop signal has to be described. The open loop signal consists of the transfer function of the aircraft due to control surface input sensed at the inertia measuring unit (rates and accelerations) and at the flow sensors, and the transfer function of the ASD and FCS from the sensor to the opening point and from the opening point to the actuators.
The individual transfer function can be derived from two different methods the first using the analytical dynamic model calculation, the second using on ground measured sensor to actuator input transfer functions from the structural coupling test superimposed with calculated magnitudes of unsteady aerodynamic transfer functions. The applicability of the analytical dynamic model calculation depends on the accuracy of the modeling and its verification. Both methods depend on the accuracy of the unsteady aerodynamic transfer functions which are in both methods derived from theoretical predictions of unsteady aerodynamics for elastic modes and control surface deflection.

Analytical Model of the Flexible Aircraft with Flight Control System

The analytical model of the flexible aircraft with ASD and FCS consists of the linear dynamic description of the flight mechanic equations of motion, the description of the flexible aircraft through modal description using generalized coordinates, generalized masses, stiffness and model structural damping and generalized aerodynamic forces of the

flexible modes and generalized control surface inertia and unsteady aerodynamic terms or generalized piezo actuator forces, the ASD and FCS is described through linear differential equations. In addition hardware and software, i.e. all sensors, actuators, computer characteristics are described by differential equations. The flexible aircraft with FCS can be demonstrated in a matrix form.

The equations of motion for the forced dynamic response of an aeroelastic system can be written in matrix differential equation form for the aerodynamic or piezoelectric ASD systems:

$$m_r b_r^2 \begin{bmatrix} M_{qq} & M_{q\delta} \\ M_{\delta q} & M_{\delta\delta} \end{bmatrix} \begin{Bmatrix} \ddot{q} \\ \ddot{\delta} \end{Bmatrix} +$$

$$+\frac{s_R}{kV}\left\{ \omega_r^2 m_r b_r^2 \begin{bmatrix} gK_{qq} & 0 \\ 0 & K''_{\delta\delta} \end{bmatrix} + \frac{\rho}{2} V^2 F s_R \frac{b_r}{S_R} \begin{bmatrix} C''_{qq} & C''_{q\delta} \\ C''_{\delta q} & C''_{\delta\delta} \end{bmatrix} \right\} \begin{Bmatrix} \dot{q} \\ \dot{\delta} \end{Bmatrix} +$$

$$+\left\{ \omega^2 m_r b_r^2 \begin{bmatrix} K_{qq} & 0 \\ 0 & K'_{\delta\delta} \end{bmatrix} + \frac{\rho}{2} V^2 F s_R \frac{b_r}{s_R} \begin{bmatrix} C'_{qq} & C'_{q\delta} \\ C'_{\delta q} & C'_{\delta\delta} \end{bmatrix} \right\} \begin{Bmatrix} q \\ \delta \end{Bmatrix} = \{Q(t)\}$$

The generalized mass and stiffness matrices are calculated using a finite element model (FEM) of the total aircraft. For dynamic response calculation the FEM is reduced to representative generalized dynamic DOF`s. The true airspeed V and semi span s_R of the reference plane are used to form the reduced frequency k = (ωs_R)/V. F is the area of reference plane and g is the structural damping of the elastic modes. The generalized forces Q(t) are equal to zero for the conventional flutter problem. The generalized coordinate q describes the amplitude of the elastic airplane modes including elastic control surface modes for a system with actuators whereas δ_0 denotes the rotation of the rigid control deflection according to the complex actuator stiffness represented by the impedance function of equation (2).

$$K_{\delta_0\delta_0} = K'_{\delta_0\delta_0} + iK''_{\delta_0\delta_0}$$

For the ASD and FCS controlled aircraft the induced control deflection $\Delta\delta$ has to be introduced as an additional degree of freedom for each control surface or piezo actuator.

The generalized forces generated by the induced control deflections $\Delta\delta$ can be described as the right-hand term of equation (1) for aerodynamic control surfaces and for piezo actuators by

$$\{Q(t)\} = -m_b b_r^2 \begin{Bmatrix} M_{q\Delta\delta} \\ M_{\delta_0\Delta\delta} \end{Bmatrix} \Delta\ddot{\delta} - \frac{\rho}{2} V^2 F s_R \frac{b_r^2}{s_R^2} \frac{s_R}{k \cdot V} \begin{Bmatrix} C''_{q\Delta\delta} \\ C''_{\delta_0\Delta\delta} \end{Bmatrix} \Delta\dot{\delta} -$$

$$-\frac{\rho}{2} V^2 F s_R \frac{b_r^2}{s_R^2} \begin{Bmatrix} C'_{q\Delta\delta} \\ C'_{\delta_0\Delta\delta} \end{Bmatrix} \Delta\delta$$

Assuming normalized rigid control surface modes or piezo actuator mode δ_0 and $\Delta\delta$, the deflection of each control surface or piezo actuator can be superimposed by

$$\delta = \delta_0 + \Delta\delta$$

δ is used here as abbreviation for rudder, and differential inboard and outboard flap or piezo actuator deflection.
The state-space-description of (1) is as follows:

$$\{\dot{x}\} = [A]\{x\} + [B]\{x\}$$

The matrix in equation (1) describing the flexible aircraft with ASD and FCS is enlarged by linearized rigid flight mechanic equations. For example the state vector for lateral control includes then rigid aircraft state variables

$$X = \lceil \beta,\ \omega_x,\ \omega_z,\ \varphi,\ \psi,\ \xi,\ \zeta,\ \varepsilon,\ r,\ q,\ d\xi/dt,\ d\zeta/dt,\ d\varepsilon/dt,\ dr/dt,\ dq/dt \rfloor$$

The flight mechanic equations may in a first approximation contain elastified aerodynamic derivatives as function of incidence, Mach number and they are for low frequency assumed to be decoupled from the flexible aircraft equations. In another approximation the flight mechanic equations are fully rigid and theoretical inertia and unsteady aerodynamic coefficients are introduced.
The flight mechanic equations for lateral control are described below:

Rigid aircraft equations,

Side Force equation

$$\left[-mV + \frac{\rho}{2} V^2 F s / V c_{y\dot{\beta}} \right] \dot{\beta} + \frac{\rho}{2} V^2 F c_{\beta} \beta +$$

$$+\left[-mV \sin\alpha_0 - \frac{\rho}{2} V^2 F s / V c_{yp} \right] \omega_x +$$

$$+\left[mV \cos\alpha_0 - \frac{\rho}{2} U^2 F s / V c_{yr} \right] \omega_z - mg \cos\alpha_0 \varphi = \tilde{Y}(t)$$

Roll Moment equation

$$\frac{\rho}{2} V^2 F s^2 / V c_{l\dot{\beta}} \dot{\beta} + \frac{\rho}{2} V^2 F s c_{l\beta} \beta - \frac{\rho}{2} V^2 F s^2 / V c_{lp} \omega_x -$$

$$-\frac{\rho}{2} V^2 F s^2 / V c_{lr} \omega_z - I_x \dot{\omega}_x - I_{xz} \dot{\omega}_z = \tilde{L}(t)$$

Yaw moment equation

$$\frac{\rho}{2} V^2 F s^2 / V c_{n\dot{\beta}} \dot{\beta} + \frac{\rho}{2} V^2 F c_{l\beta} \beta - \frac{\rho}{2} V^2 F s^2 / V c_{np} \omega_x -$$

$$-\frac{\rho}{2} V^2 F s^2 / V c_{nr} \omega_z - I_{xz} \dot{\omega}_x + I_z \dot{\omega}_z = \tilde{N}(t)$$

MODELING

Structural Modeling

Consideration of the full travel of the flexible mode frequencies with flight condition, fuel contents and actuator failure cases is necessary. The minimum experienced structural damping shall be applied. In order to be accurate, the analytical model has to be updated from ground resonance test results mainly with respect to mode frequencies.

In addition the aircraft identification test results from structural coupling test shall be adopted. Flexible mode frequency shifts with actuator demand amplitude shall be adapted to the modeling to represent minimum and maximum possible mode frequency.
In case of integrated piezo actuators the affected structural component FEM shall include finite element representation of the piezo actuators and corresponding interaction effects piezo to component structure. The properties of the integrated piezo structure shall be derived from coupon tests for the update of the FEM.

Unsteady Aerodynamic Modeling
The unsteady forces used in the dynamic model calculation shall be represented in a conservative manner.
The magnitude (modulus) of the unsteady forces of the flexible modes and of the control surface defection shall be predicted to represent a realistic high value for all Mach numbers and incidences. Since flow separation at higher incidences is leading to alleviation in the motion induced pressure distributions of the flexible modes and of the control surface deflections the introduction of unsteady aerodynamic forces from pure linear theory is regarded to be conservative. Special attention has to be put to transonic effects on the unsteady aerodynamic forces. The assumption of linear unsteady subsonic and supersonic aerodynamics derived by linear theory or numerical Euler code calculations Ref 10 in the linear range is believed to be conservative throughout the full flight envelope.
It shall be stated that the unsteady forces must be calculated for a number of reduced frequencies to cover the full frequency range.

The Phase of the unsteady Aerodynamic forces
For the phase stabilization of low frequency flexible modes like the first wing/fin bending the unsteady aerodynamic phase shall be represented in a conservative manner. A reasonable approach for the phase of the first elastic mode is again the application of linear theory. The argumentation is that at high incidence and combined high FCS gains the aerodynamic damping is increased compared to low incidence from experience found for different wing configurations. In terms of phase stability margin Ref. 3 explains the difference in a Nichols diagram, where linear theory shows the more critical condition.

FCS Model
In order to design in a robust manner the calculation of open loop transfer functions shall consider the worst ASD and FCS gain conditions. The worst trimmed end to end gain conditions have to be included into the model calculations.

Ground Test Results
Ground vibration test results and structural coupling tests are needed to verify or update the calculated results from dynamic model predictions. In general the total aircraft structural dynamic model consisting of sub components can be refined by updating the sub component stiffness and damping using the results from component ground resonance tests and aircraft ground resonance and structural coupling tests. The update of the analytical model is described in Ref. 6.

Flight Test Results
Flight test results from structural coupling/flutter tests are needed to verify or update the predicted results of open loop frequency response functions by the update of unsteady aerodynamic forces used in the dynamic model. This can be achieved through the comparison of predicted and flight test measured closed loop converted into open loop frequency transfer functions.
The comparison there is not only restricted to loop signals, also predicted accelerations at significant aircraft locations are compared, i.e. outer wing, front, rear fuselage, upper fin.
The flight test results are derived through frequency sweep excitation of the control surfaces or of the integrated piezo actuators or piezo-interface, which should be possible through a special software in the FCC's.

EXAMPLES AND RESULTS

Analytical investigations have been performed for the different ASD concepts using the analytical model of a total modern fighter aircraft including a description of ASD and FCS. Open loop frequency response calculations have been calculated first for the different systems with normalized ADS gains and filters as design input for the ASD gain and filter optimization. A first preliminary ASD control law optimization was performed for the aerodynamic systems (rudder and auxiliary rudder concept) and ASD closed loop calculations have been carried out after definition of ASD gains and filters in order to demonstrate the effects of ASD in comparison to the aircraft without ASD. For the integrated piezo system and the piezo interface only the excitation of the aircraft via piezo actuators was investigated until now, an ASD optimization for these systems will be available soon. Since all investigation of the different systems is based on the same analytical model, the results achieved can directly be compared. The inputs for generalized integrated piezos and the generalized piezo interface forces which are used here for the excitation of the total aircraft have been generated by EADS, for the piezo interface. The generalized piezo forces are derived from analytical model calculation of the fin component which includes a FEM representation of the integrated piezo actuators.
Fig. 1 shows for example the aircraft with integrated piezo actuators. The flight control computer will include the ASD control laws besides the FCS control laws. The sensors system for ASD is based on IMU signal together with accelerometer signals on the fin

Results of Rudder Concept

The block diagram for the rudder concept is demonstrated in Fig. 2. Besides the feedback loops necessary for FCS the diagram shows the lateral acceleration feedback to the rudder from fuselage and fin for the ASD.

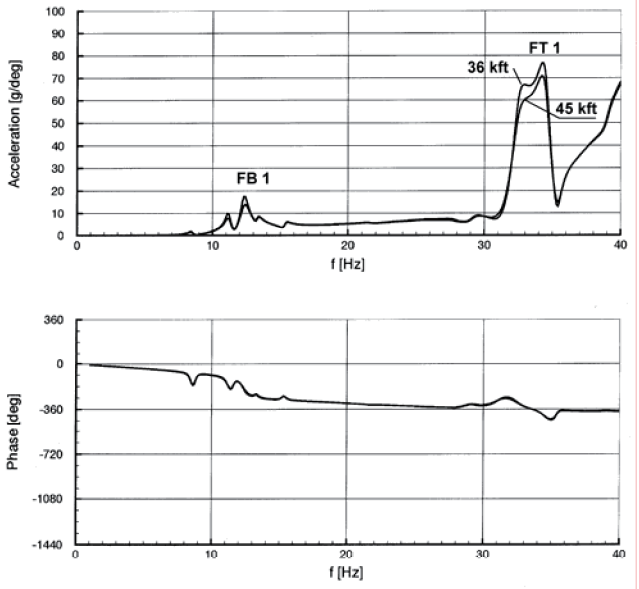

Figure 3: Open loop frequency response: Fin lateral acceleration due to rudder input; Mach = 0.8; 1g; h = 45000ft

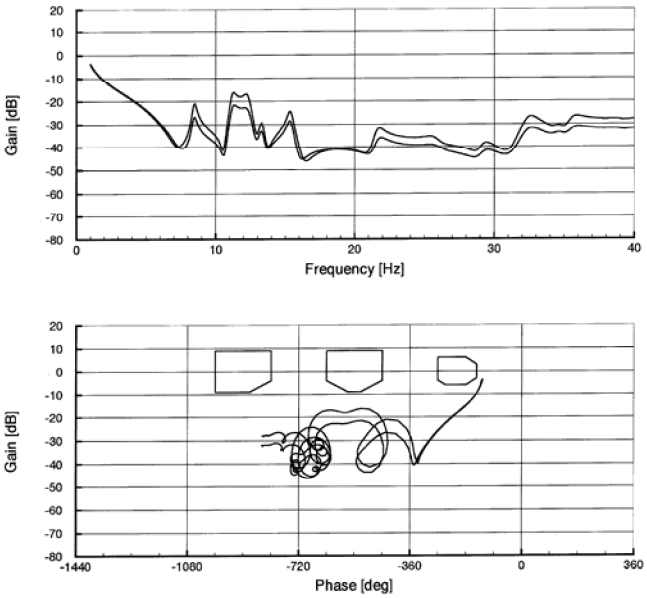

Figure 4: Open loop frequency response due to rudder input with notch filters - lateral path included; Mach = 0.8; 1g; h = 36000ft / 45000ft

Fig. 3 depicts the fin lateral acceleration open loop frequency response function due to rudder excitation for two flight conditions. The figure shows peak in the frequencies of the aircraft elastic modes:
Antisymmetric wing bending at 8 Hz, antisymmetric fuselage bending at 11 Hz, fin bending mode at 12.4 Hz and fin torsion mode at 34 Hz.

Fig. 4 and 5 demonstrates the ASD design by for Bode and Nichols plot of the open loop frequency response at the rudder breakpoint. Fig. 4 depicts the response for normalized ASD gain and Fig. 5 shows the open loop response for an ASD gain and indicates that the stability requirements are met for all elastic modes (no encroachments into the requirements for gain and phase margins). Improvements of ASD are possible by increasing the gain and still meeting the phase requirements. This step has to be performed in a safe manner, i.e. by introducing phase tolerances for actuator non-linearity.

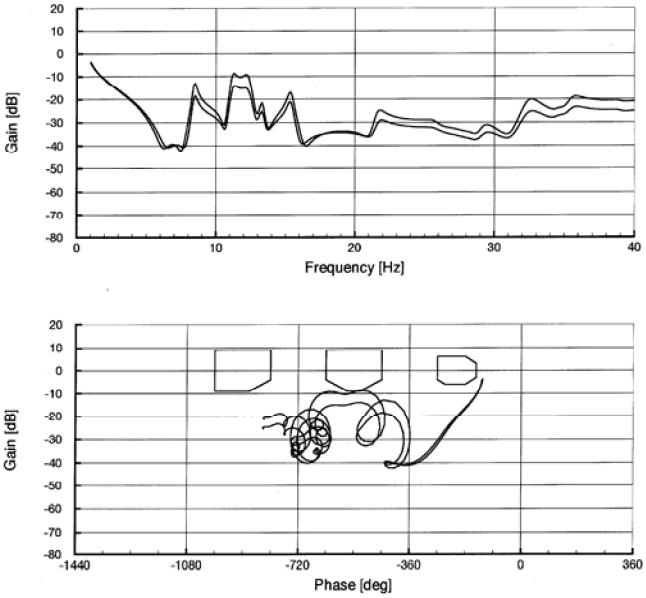

Figure 5: Open loop frequency response function due to rudder input with notch filters - lateral path included with additional gain; Mach = 0.8; 1g; h = 36000ft / 45000ft

The alleviation effect of the ASD rudder concept is demonstrated in Fig. 6, showing the comparison of fin acceleration with and without closed loop ASD. The alleviation shown can be achieved by full use of phase stabilization of the modes and using actuator maximum amplitudes still in the linear range.

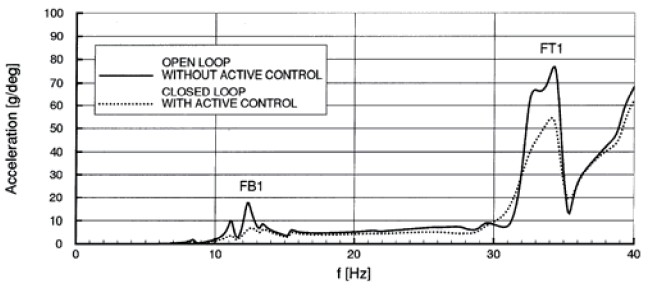

Figure 6: Open loop versus closed loop frequency response: Fin lateral acceleration due to rudder input, damping effect of active control; Mach = 0.8; 1g; h = 45000ft

Results of Auxiliary Rudder Concept

The block-diagram for the auxiliary rudder concept is demonstrated in Fig.7. Besides the feedback loops necessary for FCS the diagram shows the lateral acceleration feedback to the auxiliary rudder from fuselage and fin for the ASD.

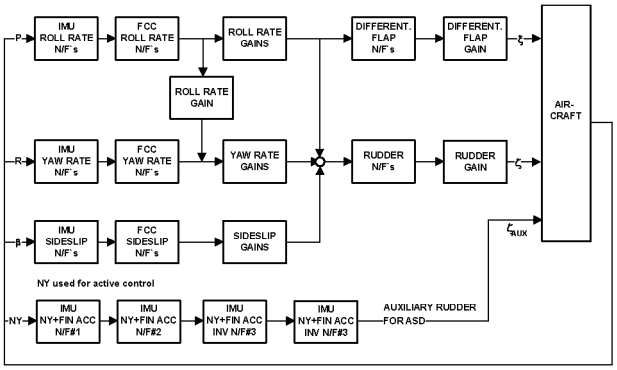

Figure 7: Control loop for ASD with auxiliary rudder

The FCS drives the full span rudder whereas the ASD drives only the auxiliary rudder (upper part of rudder).
Fig. 8 shows the comparison of the fin lateral acceleration frequency response function, FCS in closed loop, ASD in closed and open loop due to auxiliary rudder excitation. These figure shows peak in the frequencies of the aircraft elastic modes: Antisymmetric wing bending at 8 Hz, antisymmetric fuselage bending at 11 Hz, fin bending mode at 12.4 Hz and fin torsion mode at 34 Hz.

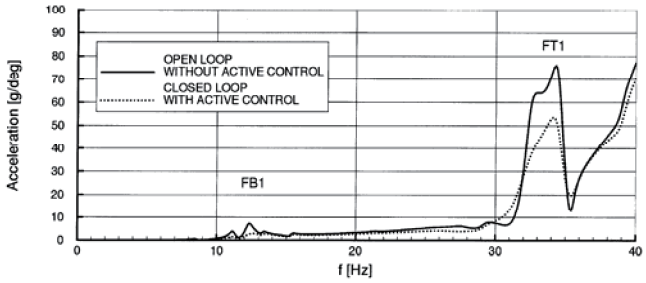

Figure 8: Open loop versus closed loop frequency response: Fin lateral acceleration due to auxiliary rudder input, damping effect of active control; Mach = 0.8; 1g; h = 45000ft

The alleviation effect of the ASD auxiliary rudder concept is demonstrated in Fig. 8, explaining the comparison of fin acceleration with and without closed loop ASD. The alleviation can be achieved by full use of phase stabilization of the modes and using actuator maximum amplitudes still in the linear range.

Results of the Integrated Surface Piezoelectric Actuator Concept

The block-diagram for the integrated surface piezo concept is demonstrated in Fig. 9. Besides the feedback loops necessary for FCS the diagram shows the lateral acceleration feedback to the piezo-actuators from fuselage and fin for the ASD.

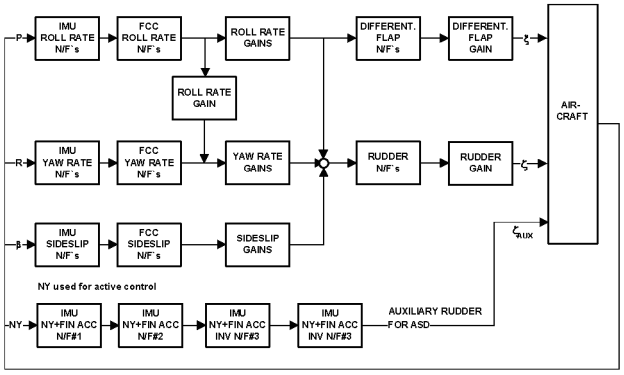

Figure 9: Flow chart of control loop with integrated piezos

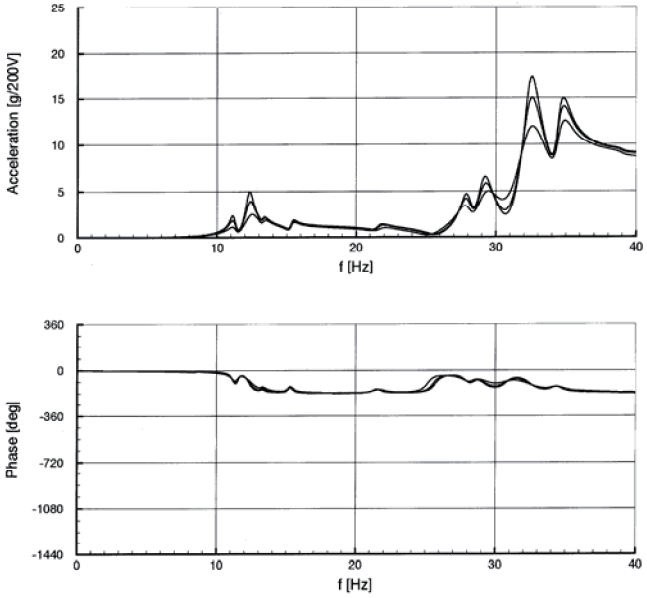

Figure 10: Open loop frequency response: Fin lateral acceleration due to integrated piezo input; Mach = 0.8; 1g; h = 21000ft / 36000ft / 45000ft; piezo input ± 200V, 600W

Fig. 10 shows the fin lateral acceleration open loop frequency response function due to piezo excitation for three flight conditions. The figure shows peak in the frequencies of the aircraft elastic modes: Antisymmetric wing bending at 8 Hz, antisymmetric fuselage bending at 11 Hz, fin bending mode at 12.4 Hz and fin torsion mode at 34 Hz.
No ASD control design has been performed yet for this system; therefore an interpretation of the result can be performed by comparison to other system open loop responses.
Fig. 10 can be compared to previous fin responses due to rudder (Fig. 3) and auxiliary rudder input (Fig. 8) in order to assess the efficiency of the piezo concept.

Results of the Interface Piezoelectric Concept

The block-diagram for the piezo interface concept is demonstrated in Fig. 9. Besides the feedback loops

necessary for FCS the diagram shows the lateral acceleration feedback to the piezo actuators from fuselage and fin for the ASD.
Fig. 11 shows the fin lateral acceleration open loop frequency response function due to piezo excitation for three flight conditions. The figure shows peak in the frequencies of the aircraft elastic modes: Antisymmetric wing bending at 8 Hz, antisymmetric fuselage bending at 11 Hz, fin bending mode at 12.4 Hz and fin torsion mode at 34 Hz.

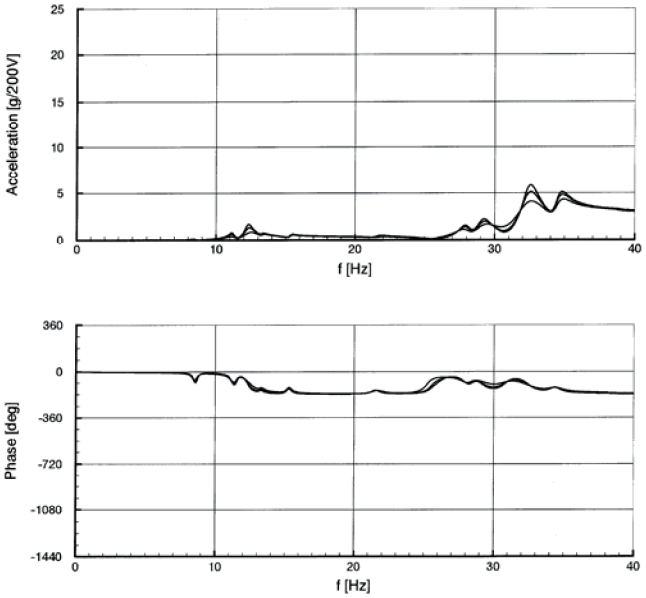

Figure 11: Open loop frequency response: Fin lateral acceleration due to piezo interface input; Mach = 0.8; 1g; h = 21000ft / 36000ft / 45000ft; piezo input ± 200V, 600W

No ASD control design has been performed yet for this system; therefore an interpretation of the result can be performed by comparison to other system open loop responses.
Fig. 11 can be compared to previous fin responses due to rudder (Fig. 3) and auxiliary rudder input (Fig. 8) in order to assess the efficiency of the piezo concept.

Comparison of the different systems

A comparison of the possible excitation of fin response due to excitation for the different systems is shown in Table 1. The comparison shows that the aerodynamic ASD systems as well as the integrated piezo system show similar excitation levels in the frequency range considered. The interface piezo concept shows less excitation. The comparison is performed on the basis of maximum actuator amplitude and max. Volt input at the same level of applied energy.

VALIDATION OF THE TOTAL AIRCRAFT MODEL

The analytical model for the present investigation is validated by on ground test and flight test results.

The validation was based on comparisons of predicted and measured on ground GRT and structural coupling test results on ground and in flight. Further validation is needed for the auxiliary rudder concept; this will be performed on a total aircraft wind tunnel model. Further validation is also needed for the modeling of integrated piezo concept and of the interface piezo concept. This validation will be performed in a first step on an already existing test box which simulates the aircraft fin structure.

Comparison of max. excitation of fin tip acceleration for fin bending mode (12.3 Hz)

CONCEPT	FIN TIP acceleration	POWER [kW]
Rudder	7.2 g / 2 deg (2 deg. Actuator limit)	2 kW
Auxiliary Rudder	9.0 g / 3 deg.	2 kW
Surface Piezo	10 g / 200 V (200V → max)	2 kW max Power
Interface Piezo	3.2 g / 200 V (200V → max)	2 kW max Power

Comparison of max. excitation of fin tip acceleration for fin torsion mode (34 Hz)

CONCEPT	FIN TIP acceleration	POWER [kW]
Rudder	20 g / 0.25 deg. (2 deg. Actuator limit)	2 kW
Auxiliary Rudder	20 g / 0.25 deg.	2 kW
Surface Piezo	34 g / 200 V (200V → max)	2 kW max Power
Interface Piezo	35.8 g / 200 V (200V → max)	2 kW max Power

Table 1: Comparison of the different concepts, Mach = 0.8; h = 45000ft, 1g;

CONCLUSION, vibration alleviation system

The present total flexible aircraft investigations performed for the different adaptive vibration alleviation system, the ruder and auxiliary rudder concept, the integrated surface piezo and the piezo-interface concept came to the following results:

- The analytically investigated different adaptive vibration alleviation systems rudder, auxiliary rudder and integrated piezo concept show similar high vibration alleviation at the aircraft fin related to equivalent power of the systems.

- The piezo interface system shows less alleviation at the moment.
- The results presented for integrated surface piezo and piezo interface concept as well as the auxiliary rudder concept have to be verified through already prepared test box tests and wind tunnel test in case of auxiliary rudder.
- Investigations shall be performed to detail the achievable alleviation of the systems in relation to maximum buffet induced vibrations for different subsonic flight conditions.

INTRODUCTION, second part

In the past decade EADS Military Air System division has investigated also different concepts for actively / adaptive deformable aircraft wing structures as part of its investigation on future structural concepts [8, 13]. Through the control of the local wing twist and camber the optimum local deformation can be achieved also with consideration of controlled aeroelastic deformations.

Besides the investigation of structural concepts, aerodynamic research programs had been initiated in order to demonstrate and validate the benefits with respect to maneuver performance, drag reduction, enhancement of aircraft maneuver control and aircraft stabilization

As part of the "Advanced Aircraft Structures Program", feasibility studies of different structural concepts of active wings have been performed. These studies have revealed significant problems related to system complexity and functionality under environmental conditions and severe problems combined with the development of adequate materials. However, promising approaches have been identified

AERODYNAMIC INVESTIGATIONS

Recently performed aerodynamic investigations of adaptive deformable aircraft structures featuring optimum aerodynamic shape control of outer wing and leading and trailing edge on a scale model of an actual aircraft have been performed with aerodynamic CFD simulations and wind tunnel tests on a complete aircraft with different shapes of the wing trailing edge, see Fig. 12.

Aeroelastic simulations, i.e. coupled structural dynamic response and computational fluid dynamics (CFD) at trimmed flight conditions, have been carried out using the dynamic model of a total aircraft trimmed both with conventional trailing edge flap deflections and with adaptive trailing edge. The calculations have been performed at high dynamic pressure assuming that the adaptive trailing edge has similar torsional stiffness compared to the conventional flap. From the simulation elastified pitch moment derivatives for the inboard and outboard trailing edge deflection have been derived which show a considerable increase in the moment derivatives. This gives an indication of the enhancement the adaptive trailing edge provides on control performance w.r.t. maneuvering and aircraft stabilization.

Figure 12: Wind tunnel test of a fighter aircraft model with simulated adaptive trailing edges.

The wind tunnel measurements have been performed on a complete aircraft model with conventional trailing edge flaps and an adaptive trailing edge in the low speed wind tunnel of the Technical University of Munich (TUM) 11-12]. The adaptive trailing edge was simulated by several rigid trailing edges for different deflections. The model support allowed measurement of total aircraft model lift, drag, pitch and roll moment. From the measurement results, considerable improvements could be demonstrated of the adaptive trailing edge as follows:

- Considerable drag reduction
- Improvement of pitch control at different lift conditions.
- Improvement of roll control at different lift conditions.

STRUCTURAL CONCEPTS

Primarily as part of the "Advanced Aircraft Structures Program" [10], different structural concepts of active wings have been investigated at EADS during the last decade.

Shape memory alloy (SMA) trailing edge

Very early, a first demonstrator (see Fig.13) of an active airfoil trailing edge has been built and tested [8]. In this approach, a network of shape memory alloy (SMA) wires stabilizes a glass fiber reinforced plastic (GFRP) structure. By sequentially contracting

counter-acting SMA wire actuators, upward and downward deflections of the trailing edge can be achieved. At a length of 200 mm, a deflection of ±25 mm was demonstrated. Beside this, the structure was able to carry all the necessary aerodynamic loads.

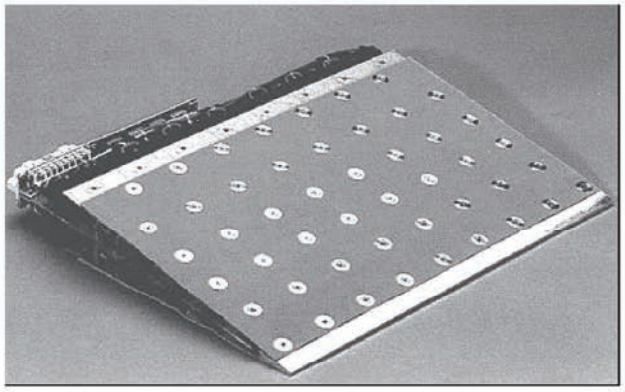

Figure 13: Trailing edge demonstrator with GFRP structure and SMA wire actuators.

Unfortunately, there are some drawbacks of the SMA wire approach, which, at the end, lead to the cancellation of the program:

- The energy efficiency of the SMA actuating system is poor.
- The SMA wire actuators are comparably slow; movement cycles are far below 1 Hz. Therefore, SMA wire actuators are not suitable for the movement of control surfaces.
- Due to the different tensile modulus in the martensitic and austenitic state, a spring back occurs if the heating circuit is switched off.

External actuator concept

The active wing program starting in 2000, investigated new concepts for active wings. The SMA active wing had demonstrated both that smart actuators where not yet ready for the task, and that a major focus has to lie on the structural concept. Therefore, the principal idea of the active wing program was to find an efficient structural design, which can be coupled to more or less conventional actuators.

The final designs had two external actuators installed in extensions of already existing pylons, Fig 14. This approach resulted in optimum actuator efficiency while minimizing additional drag. To account for the different elongation between top and bottom skin, the upper and lower skins have been joined together using flexible stringers. At the trailing edge, both skins were sliding relative to each other. This approach resulted in an extremely complex structural design, which lead to weight and cost drawbacks.

Intensive tests have been performed on flexible stringers, see Fig.15. Dynamic testing has demonstrated sufficient fatigue life, but the available translational range limits the application to the forward part of the flexible trailing edge.

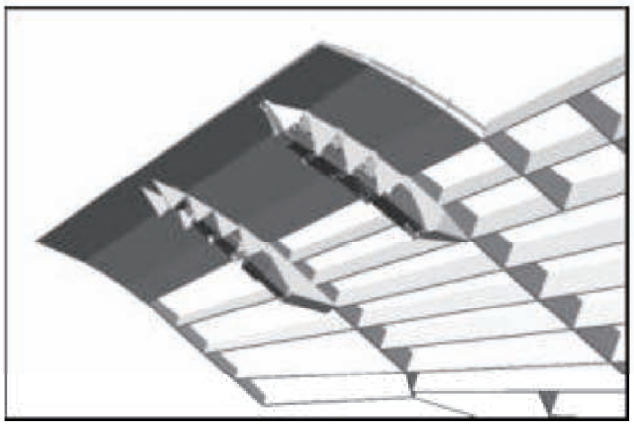

Figure 14: Design of an active wing with a flexible structure and external actuators. The external actuators are installed in extensions of already existing pylons.

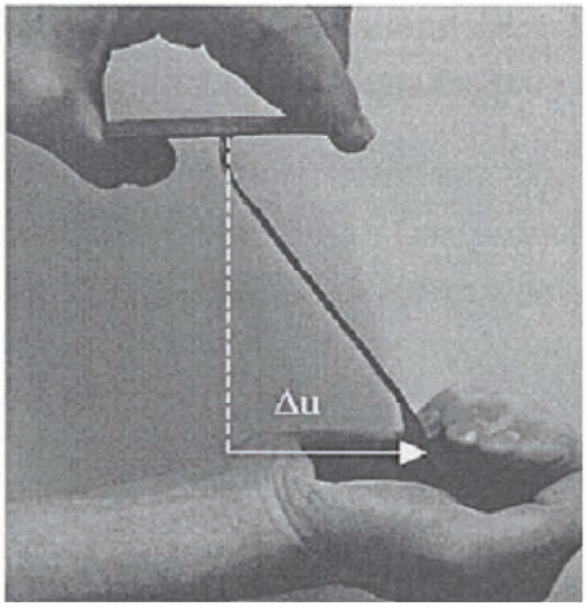

Figure 15: Structural test sample of a flexible stringer

Integrated actuator designs

At present novel concepts are under investigation that might lead to a promising way ahead. One of this concept uses torsional hydraulic actuators within the wing, another one uses transversal hydraulic actuators (patent pending), which are distributed in the aircraft skin, see Fig. 16 & 17.

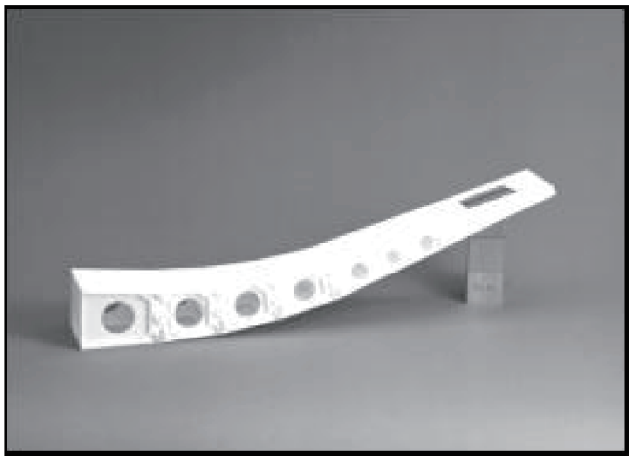

Figure 16: Mockup of the tube actuator structure with integrated actuators.

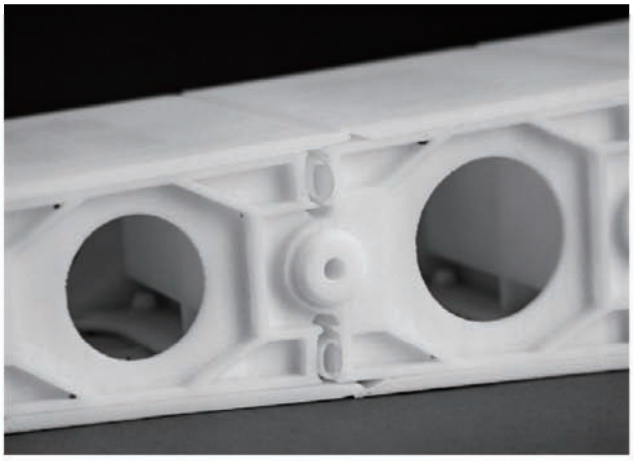

Figure 17: Detail view of a tube actuator node element mockup.

Detailed analyses of this approach have shown the potential and viability of this approach. Especially it could be shown that the expected weight increase of the adaptive wing structure including actuators is lower than the achieved overall weight decrease of the airplane due to the reduced drag. In Fig. 18, a comparison is shown for a generic fighter aircraft design, where the perceptual weight changes of the different components of the active wing are compared to a conventional wing. Despite requiring more weight for structure, actuators, hydraulics and electronics, the higher efficiency of the adaptive wing causes an overall weight decrease compared to the conventional wing.

Another interesting aspect is the reduction of power requirements. Both the torsional actuator and the tube actuator concepts are using multiple actuator lines. The moment the actuators have to counter decreases in the direction to the trailing edge, but it should be noted that the first actuator line has to counter roughly the same moment as the conventional one.

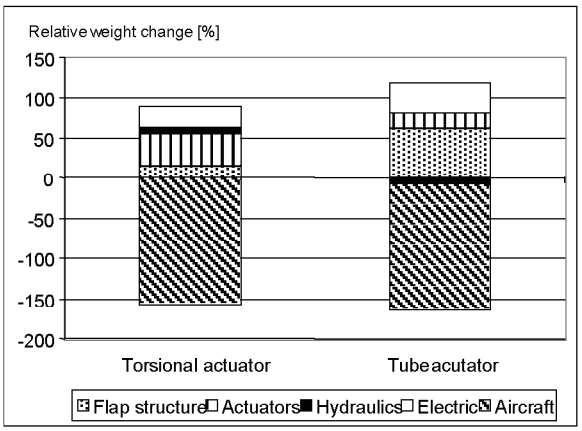

Figure 18: Weight comparison of two concepts of active wings, relative to a conventional one

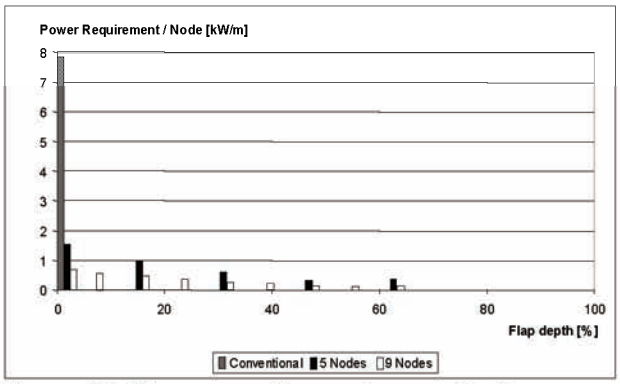

Figure 19: Power requirement per actuator for conventional (1 node), torsional actuator (5 nodes) & tube actuator (9 nodes) flap.

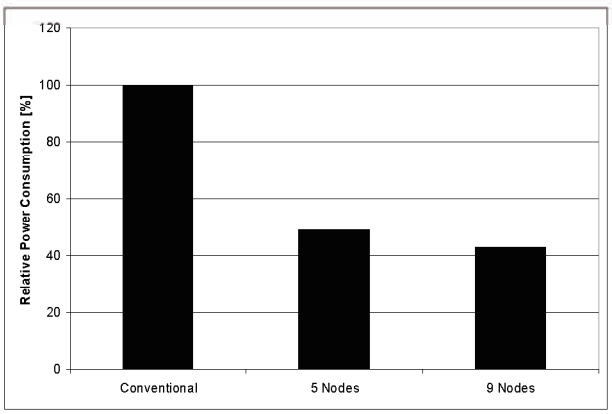

Figure 20: Total power requirement for conventional (1 node), torsional actuator (5 nodes) & tube actuator (9 nodes) flap

The difference lies in the required angular velocity at each actuator to achieve the necessary deflection within the specified time. Fig. 19 shows a comparison of the conventional, torsional actuator (with 5 nodes) and tube actuator (with 9 nodes) wing. Regarding mechanical power only, the total power requirement drops with increasing number of nodes, as shown in Fig. 20.

CONCLUSION, morphing concepts

The wind tunnel results demonstrate and validate the benefits of the adaptive trailing edge with respect to maneuver performance, drag reduction, enhancement of aircraft maneuver control and aircraft stabilization at low speed. At high dynamic pressure the improvements might reduce due to aeroelastic effects. However, as demonstrated by aeroelastic simulations there are still significant benefits available.

Structural concepts like the tube actuator concept and the torsional actuator concept have been developed that actually are capable of sustaining the structural loads and still perform the desired shape deformation. The weight of the trailing edge itself is considerably higher than that of a conventional trailing edge. However, this is more that compensated for by the improved efficiency of the wing, resulting in an overall weight reduction on aircraft level.

An interesting aspect is the reduced mechanical power requirement of the adaptive wing. As the movement of the wing is spread over a couple of actuators each performing a fraction of the movement, the total power consumption is actually lower compared to the conventional trailing edge.

The investigations have shown the potential of the concept of an adaptive wing; however a lot of development work is still necessary until an implementation of this concept can be considered.

REFERENCES

[1] A. Lotze, O. Sensburg and M. Kühn
Flutter Investigations on a Combat Aircraft with a Command and Stability Augmentation System AIAA Paper No. 75-1025, AIAA 1975 Aircraft Systems and Technology Meeting, Los Angeles

[2] O. Sensburg, J. Becker, H. Hönlinger
Active Control of Flutter and vibrations of an Aircraft.
Proceedings of the International IUTAM, Symposium on Structural Control, university of Waterloo, Ontario, Canada, June 1979

[3] W. Luber; J. Becker
High Incidence Unsteady Aerodynamic for Aeroservoelasticity Predictions
85th AGARD Structures and Material Panel Specialist Meeting, Aalborg, Denmark, October 1997

[4] H. Hönlinger, H. Zimmermann, O. Sensburg, J. Becker
Structural Aspects of Active Control Technology
AGARD Conference Proceedings on Active Control Technology, FMP Symposium Turin, Italy, May 1994
AGARD SMP Meeting on Advanced Aeroservoelastic Testing, Rotterdam, NL, May 1995.

[5] J. Becker, W. Luber
Unsteady Aerodynamic Forces at High Incidence and their Application in Structural- and Flight Control Design. International Forum on Aeroelasticity and Structural Dynamics; Manchester, UK; June 1995

(6) J. Becker, .V. Vaccaro
Aeroservoelastic Design, Test verification and Clearance of an Advanced Flight Control System. AGARD SMP Specialist Meeting on Advanced Aeroservoelastic Testing, Rotterdam, May 1995

[7] Ch. Breitsamter
Turbulente Strömungsstrukturen an Flugzeug konfigurationen mit Vorderkantenwirbeln Dissertation TUM 1997

[8] K. Dittrich,
Prospects of Smart Structures for Future Aircraft"; NATO Advanced Study Institute „Mechanics of Composite Materials and Structures"; Tróia, Portugal, July 12-24, 1998.

[9] J. Becker et al.,
The Advanced Aircraft Structures Program - An Overview", Proceedings of the SPIE smart structures conference, Newport Beach, USA, 1999.

[10] K. Dittrich,
Formveränderung von Flügel Strukturen mittels integrierter Shape Memory Alloy Aktuatoren Proceedings of the DGLR conference, Erlangen, Germany, 1994

[11] Ch. Breitsamter,
Aerodynamik hochmanövrierfähiger Flugzeuge mit formvariablen Hinterkantenklappen,
DGLR annual conference, Germany, 2003

[12] Ch. Breitsamter,
Aerodynamic Efficency of high maneuverable aircraft applying adaptive wing trailing edge section, 24th International Congress of the Aeronautical Sciences, 2004.

[13] K. Dittrich, J. Becker, W. Luber
Structural Concepts for Morphing Wing
Third European Conference on Structural Control, 2004 Vienna, Austria